Pergamon

Int. J. Heat Mass Transfer. Vol. 39, No. 14, pp. 2853–2860, 1996

0017-9310/96 $15.00 + 0.00

0017-9310(95)00389-4

g-Jitter induced free convection in a transverse magnetic field

BEN Q. LI

Department of Mechanical Engineering, Louisiana State University, Baton Rouge, LA 70803, U.S.A.

(*Received* 21 *April* 1995 *and in final form* 9 *November* 1995)

Abstract—This paper reports an analytical analysis of g-jitter induced flows in microgravity under the influence of a transverse magnetic field. The analysis is carried out for a simple system consisting of two parallel plates held at different temperatures. A single component of time harmonic g-jitter is considered. General solutions are obtained for the velocity profile with a combined effect of oscillating g-jitter driving force and induced Lorentz force, the latter resulting from an application of a transverse magnetic field. Various limiting cases are examined based on the general solutions. Detailed calculations are also provided. Results show that the g-jitter frequency, applied magnetic fields and temperature gradients all contribute to affect the convective flow. It is found that the amplitude of the velocity decreases at a rate inversely proportional to the g-jitter frequency and with increase in the applied magnetic field. The induced flow oscillates at the same frequency as the affecting g-jitter, but out of a phase angle. The phase angle is a function of geometry, applied magnetic field, temperature gradient and frequency. While a magnetic field can be applied to suppress oscillating flows associated with g-jitter, it is more effective in damping low frequency flows but only has a moderate damping effect on the flow induced by high frequency g-jitter. The temperature gradient also has a profound effect on the g-jitter induced flow. The oscillating velocity profile evolves from a single wave to a half wave across the channel and the maximum magnitude of the velocity increases as much as a factor of three as the wall temperature parameter increases. The wall electric conditions also affect the flows and stronger damping effects occur when the walls are electrically conducting.

1. INTRODUCTION

Natural convection is driven by buoyancy forces resulting from both temperature gradient and gravity field. This convective flow is known to have a profound effect on the solutal homogeneity of crystals grown from melt on earthbound conditions. Much of the interest in going to space to carry out the melt growth of semiconductor or metal crystals is to reduce this buoyancy driven convection through significant reduction in gravity. While microgravity environment is indeed helpful in suppressing convective flows, it introduces additional effects that are undetectable or present during Earth-based growth of crystals. One of these effects that affects the melt growth experiments is the flow associated with residual accelerations or g-jitter. Flight experiments unveiled that residual accelerations or g-jitter occurring during space processing can cause appreciable convective flows in the melt pool, making it difficult to realize a diffusion controlled growth from melts in microgravity, as originally intended [1].

The residual accelerations associated with microgravity come from crew motions, mechanical vibrations (pumps, motors, excitations of natural frequencies of spacecraft structures), spacecraft manoeuvres and attitude, atmosphere drag and the Earth's gravity gradient [2]. Studies on g-jitter effects showed that convection in microgravity is related to the magnitude of g-jitter and to the alignment of the gravity field with respect to the growth direction or the direction of the temperature gradient [3–5]. A residual gravity of 10^{-5}–$10^{-6}\,g$ is found to be sufficient to cause unacceptable fluid motion in the liquid, unacceptable in the sense that the g-jitter induced flow is intensive enough to affect deleteriously the solutal element distributions in the melt and hence the quality of the crystals grown. The orientation of the gravity vector with respect to the temperature gradient plays also an important role in melt flows. The velocity attains a maximum when the gravity vector is perpendicular to the temperature gradient.

Numerous attempts have been made to estimate and calculate the adverse effects of time varying g-jitter [6–11]. These calculations are all based on numerical models. Both 2D and 3D numerical models have been developed for this purpose [4, 12]. These models have been used to study the effects associated with both idealized single- and multiple-frequency g-jitter modulations and realistic g-jitter data collected by accelerometer during actual flight experiments. These studies showed that the frequency, amplitude and spatial orientation of the residual gravity vector all play an important role in determining the convective flow behavior of the system. When the residual accelerations oscillate about the positive and negative of an axis, the orientation of this direction relative to the density gradient determines whether a mean flow

NOMENCLATURE

$\mathbf{B}$	magnetic induction
B_0	applied magnetic field
E	nondimensionalized electric field, $E = E_z/E_0$
E_0	electric field scale
$g(t)$	g-jitter or residual gravity field
g_0	magnitude of g-jitter
Ha	Hartmann number, $Ha = LB_0\sqrt{(\sigma/\nu\rho)}$
I	total current
j	pure imaginary number, $\mathrm{j} = \sqrt{-1}$
J	current density
$\mathfrak{J}$	nondimensionalized current density
L	width of the channel
Re_m	magnetic Reynolds number, $Re_m = u_0 L\sigma\mu$
r_T	nondimensionalized wall temperature parameter, $r_T = (T_1 - T_0)/(T_2 - T_0)$
T, T_1, T_2, T_0	temperature, temperatures of wall 1, wall 2 and fluid
t	time
u	velocity
u_0	velocity scale
U	nondimensionalized velocity, a complex quantity
$\|U\|$	amplitude of velocity, $U\| = \sqrt{(U \cdot U^*)}$
$\hat{\mathbf{x}}$	unit vector in the x-direction
$\hat{\mathbf{y}}$	unit vector in the y-direction
y	y-coordinate
Y	nondimensionalized y coordinate, y/L
z	z-coordinate.

Greek symbols

β	system parameter, $\beta = \sqrt{(Ha^2 + \mathrm{j}\Omega)}$
β_T	thermal expansion
σ	electrical conductivity
δ	electromagnetic skin depth
ρ	density
μ	magnetic permeability of free space
ν	kinematic viscosity
ω	applied frequency
Ω	nondimensionalized frequency, $\Omega = \omega L^2/\nu$
θ	nondimensionalized temperature, $\theta = (T - T_0)/T_2 - T_0)$
τ	nondimensionalized time, $\tau = t/\tau_0$
τ_0	time scale, $\tau_0 = L^2/\nu$.

Subscript

x, y, z	x, y and z components of a vector field
T	temperature.

is generated in the system [10]. Sinusoidal oscillating accelerations induce an oscillating convective flow and composition oscillation in the liquid pool. The resultant velocity and composition fields oscillate with the same frequency as the affecting gravity field.

Undoubtedly, these studies have shed light on the basic nature of g-jitter effects and have provided a thrust to devise useful mechanisms by which the g-jitter induced convective flows may be further suppressed. One of the untested ideas is to apply the principle of magnetic damping to achieve the velocity reduction. Magnetic damping is a less plausible mechanism than gravity for free convection reduction. It originates from the interaction of the flow field of an electrically conducting fluid and an applied magnetic field. This interaction gives rise to an opposing Lorentz force that reduces or damps the flow velocities in the liquid. Application of a magnetic field has been found to be effective in controlling the melt convection during crystal growth from melts under terrestrial conditions and has now been widely practiced in the metals and semiconductor industries [13]. While there has been a large amount of literature addressing both the basic characteristics of g-jitter induced flows and application of magnetic damping to convection control in melt growth on Earth, little, if any, work has appeared to assess the magnetic field effect on the convective flow associated with g-jitter in microgravity.

In this paper, the behavior of g-jitter induced free convection in microgravity under the influence of a transverse magnetic field is analysed for a simple system consisting of two parallel plates held at different temperatures. Our objective is to develop a basic understanding of the interaction between an applied magnetic field and oscillating flows associated with g-jitter. Towards this end, a somewhat idealised, single frequency g-jitter component is considered. From data collected from flight experiments, g-jitter can be approximated using a Fourier series, with each component oscillating time harmonically. Thus, the total effect of g-jitter may be considered as a superposition of the effects caused by each individual component for the system being considered. It is noted that the superposition may not be possible for general flow systems involving nonlinear terms. In what follows, general solutions are obtained first for the velocity profile with a combined effect of oscillating g-jitter driving force and induced Lorentz force resulting from an application of a transverse magnetic field. Various limiting cases are then examined based on the general solution. Detailed calculations are also presented. g-Jitter induced flow is studied as a function of various parameters including g-jitter frequency, applied mag-

netic fields, temperature gradients and wall electric conditions.

2. MATHEMATICAL ANALYSIS

Let us consider a free convection problem as illustrated in Fig. 1. An electrically conducting fluid is at temperature T_0 and flows as a result of temperature gradient in between two parallel plates that are infinitely long in both x and z directions but held at different temperatures. We consider here a fully developed flow. Further we assume that the g-jitter field under consideration is spatially constant and otherwise varies time harmonically. For low Prandtl number fluids such as molten metals or semiconductor melts, which are of direct relevance to microgravity materials processing, the temperature field is primarily diffusion controlled and can be considered approximately unaffected by the free convection. Therefore, the time varying gravity field will generate an oscillatory velocity field. If a transverse DC magnetic field is imposed as shown in Fig. 1, this oscillatory flow field will be damped. The mathematical description of the problem is given by both the Maxwell equations for the electromagnetic phenomena and the Navier–Stokes equation for the fluid flow phenomena [14–16]. For the geometry shown in Fig. 1, these equations may be simplified as below,

$$-\frac{\partial E_z}{\partial y}=\frac{\partial B_x}{\partial t} \tag{1}$$

$$\frac{\partial u}{\partial t}=\nu\frac{\partial^2 u}{\partial y^2}+g(t)\beta_T(T-T_\infty)-\frac{\sigma}{\rho}(E_z+B_0u)B_0. \tag{2}$$

For experiments considered for space processing, the magnetic Reynolds number, Re_m, is very small. For example, for typical processing conditions [3], the velocity is scaled at $u\sim 0.4$ mm s^{-1} and $L=0.02$ m. Hence $Re_m\sim 1\times10^{-5}$ for silicon melts. It can be shown that for such a small Re_m and a moderate external magnetic field B_0, to a leading order, the magnitude of the induced magnetic field B_x is [14].

$$B_x\approx B_0Re_m. \tag{3}$$

Thus, in comparison with B_0, B_x can be neglected and one thus has the effective magnetic field given by

$$\mathbf{B}=B\hat{\mathbf{x}}+B\hat{\mathbf{y}}\approx B_0\hat{\mathbf{y}}+B_0Re_m\hat{\mathbf{x}}\approx B_0\hat{\mathbf{y}} \tag{4}$$

which means that the bending of the magnetic field caused by flow is negligible.

For a time harmonic g-jitter with a frequency ω, $g(t)=g_0e^{j\omega t}$, the flow field and the induced electric field should have a similar time varying behavior. Hence, equation (2) can be simplified. If the following scaling factors are chosen for the velocity, the electric field and time,

$$u_0=\frac{g_0\beta_T(T_2-T_0)L^2}{\nu}$$

$$E_0=\frac{g_0\beta_T(T_2-T_0)L^2B_0}{\nu}\qquad \tau_0=\frac{L^2}{\nu}$$

equation (2) above can be rewritten in a non-dimensionalized form as below

$$\frac{d^2U}{dY^2}-\beta^2U=Ha^2E-\theta \tag{5}$$

where $\beta=\sqrt{(Ha^2+j\Omega)}$ is a complex number.

For a time harmonic velocity field, the induced electric field and hence the induced magnetic field should vary harmonically with the same frequency. For a low frequency system, the electric field behaves approximately as if it were induced by a non-oscillating flow field, provided that Re_m is small. To see this, equation (1) is nondimensionalized using the parameters given above, and thus the spatial variation of the amplitude of E can be shown to be on the order of $Re_m(\omega L/u_0)$

$$\frac{dE}{dY}=\left(\frac{\omega L}{u_0}\right)\frac{B_x}{B_0}\approx\left(\frac{\omega L}{u_0}\right)Re_m. \tag{6}$$

Studies showed that for most experimental designs considered for space processing, the predominant effect of g-jitter effect comes from the low frequency component, in particular those within the range of 10^{-3}–10^{-2} Hz [3, 4, 10]. For this frequency range, $(\omega L/u_0)Re_m=L^2\omega\sigma\mu=(3.8\text{–}38)\times10^{-6}$. This suggests that to a leading order the electric field E may be considered uniform across the channel but otherwise varies with time harmonically with the frequency of the affecting g-jitter component.

For a low Prandtl number melt, such as a molten semiconductor or metal, the heat transfer is primarily diffusion controlled in microgravity and hence the energy equation takes the form of

$$\frac{d^2\theta}{dY^2}=0. \tag{7}$$

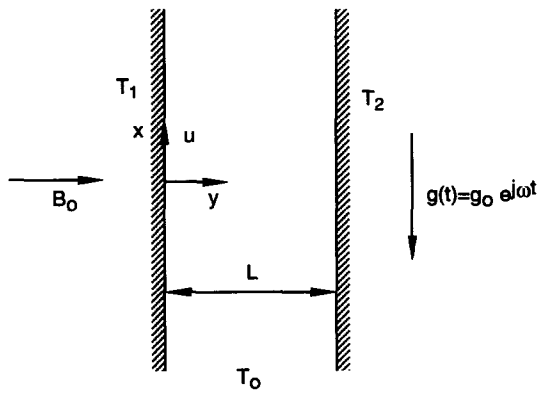

Fig. 1. Schematic representation of g-jitter induced free convection problems and coordinate system used for calculations.

This equation can be readily integrated with the following boundary conditions

$$\theta = r_T \quad \text{at } Y = 0 \quad \text{and} \quad \theta = 1 \quad \text{at } Y = 1$$

with the result for the temperature profile described by a simple linear relation

$$\theta = (1 - r_T) Y + r_T. \tag{8}$$

Knowing the temperature field, the velocity field can be calculated. Substitution of equation (8) into equation (5) and application of no slip boundary conditions along the walls result in the final velocity profile, namely

$$U = \frac{1}{\beta^2}\left[(Ha^2 E - 1)\frac{\sinh(\beta Y)}{\sinh \beta} - Ha^2 E + r_T + (1 - r_T) Y + (Ha^2 E - r_T)\frac{\sinh(\beta(1 - Y))}{\sinh \beta}\right]. \tag{9}$$

Having obtained the velocity distribution, other relevant electromagnetic quantities can be determined. The induced current density and its spatially averaged value, that is, the total current, are calculated by the following expressions,

$$\Im = E + U \tag{10}$$

$$I = \int_0^1 \Im(Y)\, dY = E + \frac{1}{\beta^2}\left[\frac{\cosh \beta - 1}{\beta \sinh \beta}(2Ha^2 E - 1 - r_T) + \frac{1 + r_T}{2} - Ha^2 E\right]. \tag{11}$$

Note that equations (9) and (11) both contain the electric field E, which must be determined by the electric conditions of the walls.

3. RESULTS AND DISCUSSION

The above analytical solutions can be applied to assess the behavior of the g-jitter induced flow with or without an applied magnetic field. Prior to discussing the detailed flow behavior, analyses of some limiting flow conditions will be presented. The analyses will allow us to derive some simplified functional relationships by which some asymptotic behavior of the flow associated with g-jitter as affected by a magnetic field may be estimated.

3.1. *Some limiting cases*

3.1.1. *Pure convection* ($\Omega = 0$ and Ha $= 0$). This is the case often reported in the literature [17, 18]. In this case, the gravity field is considered constant, or $\Omega = 0$, and no magnetic field is imposed over the convective flow. Thus, $\beta = 0$. This corresponds to the buoyancy driven flow under terrestrial conditions. The solution of the flow is imbedded in equation (9) and can be obtained by first considering the solution when β is small and then letting β approach zero.

When β is small, the hyperbolic sine function can be expanded in a Taylor series, that is,

$$\sinh \beta = \beta + \tfrac{1}{6}\beta^2 + O(\beta^3). \tag{12}$$

With this substituted into equation (9), canceling β^2 at both nominator and denominator, and then letting β approach 0, one has

$$\lim_{\beta \to 0} U = (r_T - 1)\frac{Y^3}{6} - r_T \frac{Y^2}{2} + (2r_T + 1)\frac{Y}{6} \tag{13}$$

which confirms with the expression obtained by Aung by direct solution of equation (6) with $\beta = 0$ [17]. Note that the velocity solution is real and the imaginary part becomes zero for this limiting case.

3.1.2. *Pure g-jitter induced time harmonic motion* (Ha $= 0$) *and frequency effects.* In this case, free convection is induced by g-jitter with a non-dimensionalized frequency Ω and no transverse magnetic field is applied. As a result, the Hartmann number Ha is zero. With this condition substituted in equation (9), one obtains an oscillatory flow whose amplitude is spatially dependent,

$$U = \frac{1}{j\Omega}\left[r_T + (1 - r_T) Y - \frac{\sinh(\sqrt{(j\Omega)}\, Y) + r_T \sinh(\sqrt{(j\Omega)}(1 - Y))}{\sinh \sqrt{(j\Omega)}}\right]. \tag{14}$$

From equation (14), it is clear that when the frequency goes high, the amplitude of the oscillatory flow is reduced, although the time varying behavior, or the frequency of the velocity field remains the same as the g-jitter field. The rate of this velocity reduction is inversely proportional to the frequency associated with g-jitter. For the limiting case where $\Omega \to \infty$, there exists basically no flow. This conclusion is consistent with findings reported by Alexander *et al.* who did extensive numerical simulations for a 2D cavity [3, 4].

3.1.3. *Magnetic damping of natural convection* ($\Omega = 0$) *under earthbound conditions.* This case corresponds to the application of magnetic damping effects on natural convection driven by the Earth gravity field. The velocity expression can be obtained by simply setting $\Omega = 0$ and letting $\beta = Ha$ in equation (9) with the result,

$$U = \frac{1}{Ha^2}\left[(Ha^2 E - 1)\frac{\sinh(Ha\, Y)}{\sinh Ha} - Ha^2 E + r_T + (1 - r_T) Y + (Ha^2 E - r_T)\frac{\sinh(Ha(1 - Y))}{\sinh Ha}\right]. \tag{15}$$

We note that when $r_T = 1$, the above expression

reduces to the solution of classical Hartmann problem where the flow is driven by a constant pressure gradient [16]. For this particular case, the pressure gradient would be normalized as one.

3.1.4. *Magnetic damping effect on g-jitter induced convection* ($\Omega \neq 0$). Two types of velocity can result depending on the electric conditions of the walls. When the walls are made of electrically insulating materials, there should be no net current flowing in the system, or $I = 0$. As a result of this, the electric field can be obtained from equation (11) with the result,

$$E = \frac{1+r_T}{2} \frac{2\cosh\beta - \beta\sinh\beta - 2}{[2Ha^2(\cosh\beta - 1) + j\Omega\beta\sinh\beta]}. \tag{16}$$

It should be noted that even though the total current is zero, or no net current flows out of the system, the current density is not zero. Instead, it forms a recirculating path within the melt as a result of the divergence of the current density having to be zero.

If the walls are electrically conducting or ideal conductors, the total current that can flow out of the melt will not be zero. However, the fact that the tangential electric field must be continuous across the melt to wall interface requires the electric field in the melt to be zero, or $E = 0$ [16]. In this case, the electric current is induced by the applied magnetic field and the velocity in the system and the total current flowing through the system is given by equation (11). The velocity profile for this case thus becomes,

$$U = \frac{1}{\beta^2}\left[r_T + (1-r_T)Y - \frac{\sinh(\beta Y) + r_T\sinh(\beta(1-Y))}{\sinh\beta}\right]. \tag{17}$$

For either of the two cases, one can easily see that the oscillatory convective flow can be reduced if a magnetic field is applied. For a sufficiently large magnetic field, the velocity may be reduced to the extent that the condition for a diffusion controlled growth is met. As a limiting case, zero velocity attains if β is let to approach to an infinity or $\beta \to \infty$, with Ω held constant in equations (9) and (16) for insulating walls and equation (17) for conducting walls. Since $E \sim 1/Ha$ as $Ha \to \infty$ [see equation (16)] for insulating walls, we have the following asymptotic relation as $\beta \to \infty$ for a g-jitter field,

$$U \sim \frac{1}{\beta^n} \sim \frac{1}{B_0^n} \tag{18}$$

where $n = 2$ for insulating walls and $n = 1$ for conducting walls. For $r_T = -1$, however, $n = 2$ for both insulating and conducting walls, as in this case $E = 0$ [see equation (16)]. It is worth noting that the above relation should be applicable as well to magnetic damping of non-time-harmonic free convection under terrestrial conditions.

3.2. *Detailed calculations*

Detailed flow distributions are presented in this section. Here the majority of cases presented are for conducting wall boundary conditions in the z-direction, and consequently the electric field E is set equal to zero. The afterward check on the velocity results indicated that the error in the velocity associated with neglecting the time varying contribution in equation (1) is smaller than 0.001%. The selected results presented below show the effects of g-jitter oscillating frequencies, the applied magnetic field and the temperature gradients. The results are presented in a nondimensional form. The nondimensional numbers used for calculations are obtained from properties of molten silicon and for the g-jitter component with a frequency range of 10^{-3} to 10^{-2} Hz, or

$$\Omega = \omega L^2/\nu = 2\pi(0.001\text{–}0.01) \times 0.0004/3.5 \times 10^{-7} = 7.18\text{–}71.8,$$

except for a few cases. This frequency range is considered the most influential in affecting fluid flows in space materials processing systems.

Figure 2 shows the natural convection distribution across the width of the channel induced by g-jitter without an applied magnetic field for different times. The quantity plotted along the vertical axis is Imag $(Ue^{j\Omega\tau})$ = Real$(U)\sin(\Omega\tau)$ + Imag$(U)\cos(\Omega\tau)$, which represents the measurable value for a driving force $g = \text{Imag}(g_0 e^{\Omega\tau}) = g_0\sin(\omega t)$. The flow oscillates about zero and changes direction, as expected. It is noticed that at around $\Omega\tau = 5\pi/4$ the velocity profile also oscillates along the width of the channel but for

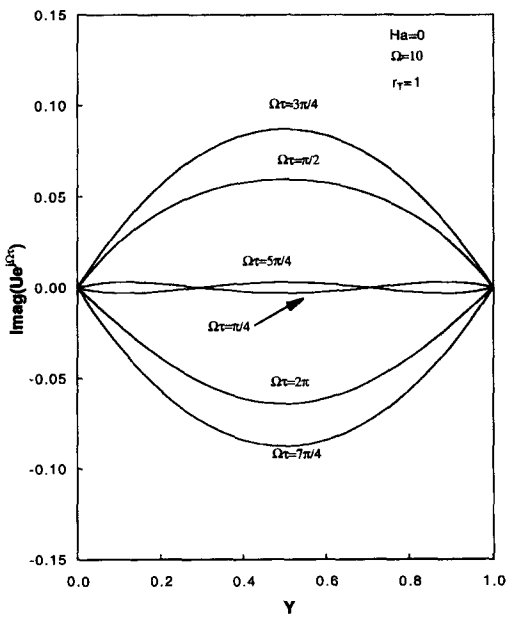

Fig. 2. Velocity distribution of oscillating free convection induced by g-jitter.

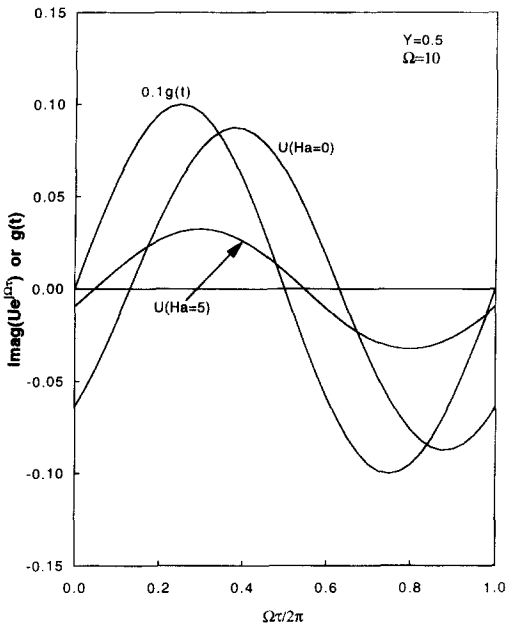

Fig. 3. g-Jitter induced free convection variation over a cycle of oscillation.

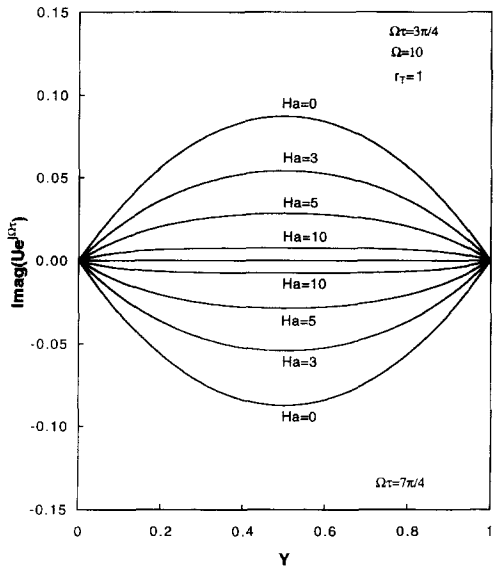

Fig. 4. Magnetic field effect on the damping of flows associated with g-jitter.

other times the velocity profile is approximately parabolic.

Figure 3 depicts the flow behavior at a fixed position ($Y = 0.5$) with and without a magnetic field. As a reference, the g-jitter oscillation driving the natural convective flow is also plotted but scaled down by a factor of 0.1 for the purpose of comparison. It is clear that the flow oscillates at the same frequency as g-jitter either with or without a magnetic field. There exists a phase change, however, between the g-jitter and the flow. The phase angle is strongly affected by the magnetic field. It is also clear from the figure that application of the magnetic field helps to suppress the flow, and the flow intensity is damped more than 50% when the Hartmann number increases from 0 to 5. The damping effect of the magnetic field on the g-jitter induced flow is further illustrated in Fig. 4, where the flow distribution is plotted as a function of the Hartmann number. As a limit, the flow can be damped entirely if a very large magnetic field is applied, as indicated by the horizontal line across $U = 0$.

The effect of the g-jitter frequency on the flow behavior with and without a magnetic field is presented in Figs. 5 and 6. As shown in Fig. 5, g-jitter induced flow decreases quickly as the frequency increases, suggesting that higher frequency g-jitter would have less harmful effects in inducing flow variation across the channel. This is consistent with our previous limiting analysis as discussed in Section 3.1.2. The flow variation across the channel with an imposed magnetic field is shown in Fig. 6. Comparison of these two figures indicates that the magnetic field can be very effective in damping flows induced by the low frequency g-jitter. In fact, it is more effective in suppressing the flows associated with g-jitter with lower frequencies. To assess this effect quantitatively, the amplitude of the induced velocity at $Y = 0.5$ is plotted as a function of Ha and frequency, as appears in Fig. 7. The magnetic field strongly affects the low frequency convective flow and only has a moderate effect on the high frequency g-jitter flows. At $Ha = 15$ and beyond, the curves converge to virtually the same line almost parallel to the horizontal axis, indicating that the frequency becomes basically irrelevant and further increase in the magnetic field would have little effect on damping the flow. This is consistent with our earlier asymptotic analyses presented in Section 3.1.4.

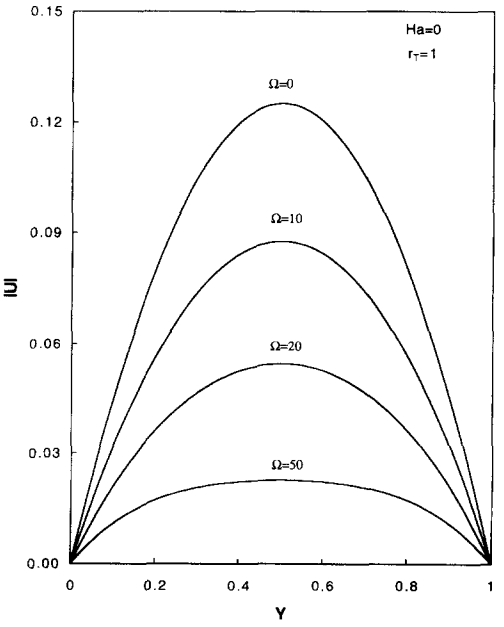

Fig. 5. g-Jitter frequency effect on oscillating free convection in a vertical channel.

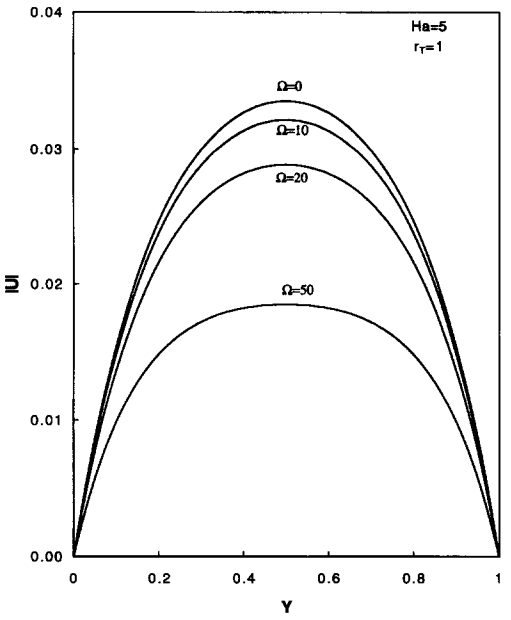

Fig. 6. Dependency of convective flows on g-jitter frequency in a magnetic field.

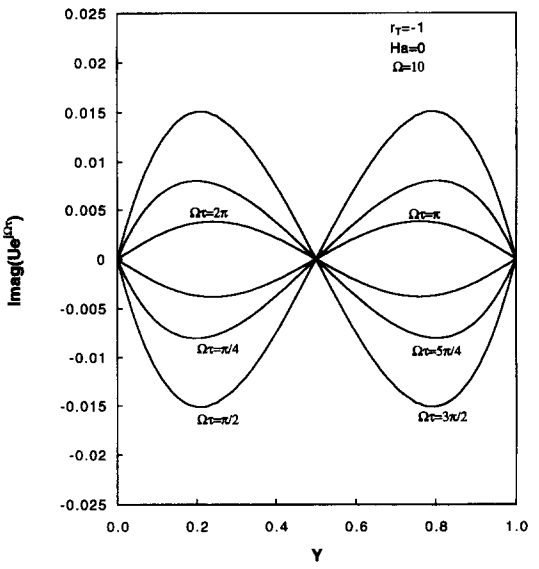

Fig. 8. Oscillating behavior of convective flows at the wall temperature parameter, $r_T = -1$.

As the flow is driven by a combination of the temperature gradient and gravity residuals (i.e. g-jitter) in microgravity environment, the temperature gradient also affects the fluid flow behavior. Figure 8 shows the flow distribution across the channel with $\Omega\tau$ as a parameter at the wall temperature parameter, $r_T = -1$. In contrast with the velocity profiles in Fig. 2, the flow at $r_T = -1$ shows a well defined wave oscillation along the Y-direction and there exists a time-invarying nodal point at $Y = 0.5$ where the velocity is equal to zero. The effect of temperature gradient on the flow is also depicted in Fig. 9. It is apparent that the velocity profile gradually approaches a half-wave shape, and also the magnitude of the velocity increases by more than a factor of 3 as r_T increases from negative 1 to positive 1.

For magnetically damped flows, the electric conditions of the walls also have an effect on the flow behavior in the channel. The results presented above are computed assuming the walls are electrically conducting. The velocity profile across the channel when the walls in the z-direction are electrically insulated is illustrated in Fig. 10. As a result, the total current flowing out of the system is zero, but the electric field is calculated by equation (16). From Figs. 5 and 10, it is clear that application of a magnetic field also

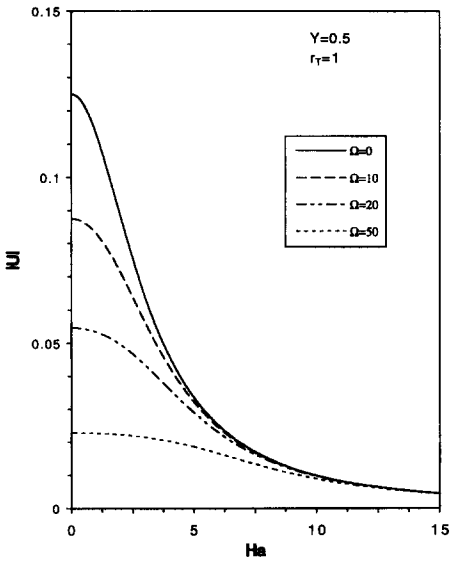

Fig. 7. Decrease of velocity amplitude $|U|$ as a function of applied magnetic field strengths.

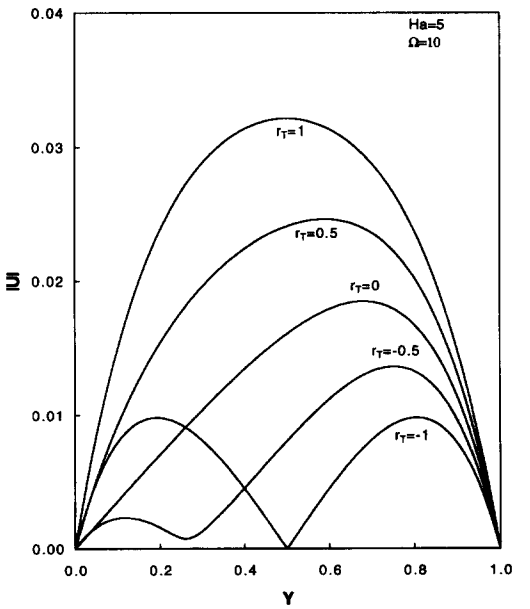

Fig. 9. Dependency of the velocity amplitude upon temperature gradients.

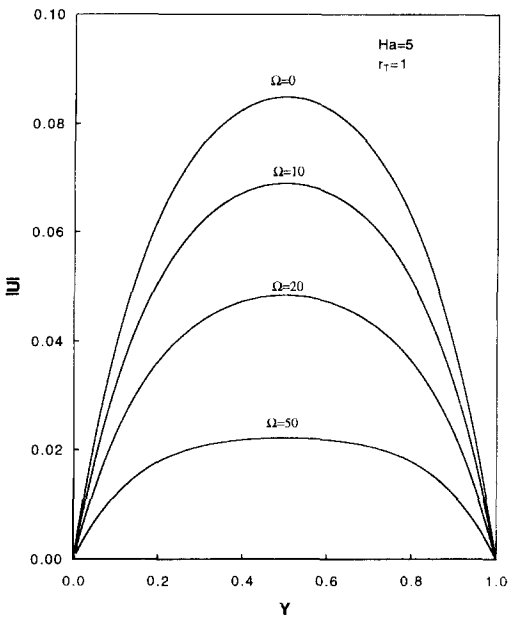

Fig. 10. Flow distribution along the y-direction with the electrically insulating walls.

results in velocity reduction with electrically insulating walls. Comparison of Figs. 6 and 10 further illustrates that the magnetic damping effect is much stronger when the walls are electrically conducting, although the velocity profiles are similar for both conducting and insulating walls. This is qualitatively consistent with the asymptotic results [see equation (18)].

4. CONCLUDING REMARKS

This paper presents an analytical analysis of g-jitter induced flow behavior in a parallel plate channel subject to a transverse magnetic field. Only single component of the g-jitter effect was considered. The parameters used in the analyses are derived from the material properties of molten silicon and correspond to the influential g-jitter frequency range reported in the literature. The study focused on the steady state, oscillating behavior of a fully developed flow in the channel. The general solution was obtained for the velocity and various limiting cases were examined. The g-jitter frequency, applied magnetic fields and temperature gradients all contribute to affect the convective flow. The detailed flow behavior was also presented as a function of applied magnetic field, oscillating frequency of g-jitter and temperature gradients. The analyses showed that the amplitude of the velocity decreases inversely proportional to the g-jitter frequency and also as the applied magnetic field increases. The induced flow oscillates at the same frequency as the affecting g-jitter, but out of a phase angle that is a function of geometry, applied magnetic field, temperature gradient and frequency. While a magnetic field can be applied to suppress oscillating flow associated with g-jitter, it is more effective in damping low frequency flows but only has a moderate damping effect on the flow induced by high frequency g-jitter. The temperature gradient also has a profound effect on the g-jitter induced flow. As the wall temperature parameter increases from -1 to 1, the magnitude of the velocity increases by a factor of three and the velocity profile evolves from a single sinusoidal wave to a half-wave shape. Also, magnetic damping is more effective with electrically conducting walls.

Acknowledgements—The author acknowledges the support of this work by NASA (grant no. NAG-81252) and NASA/LaSPACE (grant no. NGT-40039).

REFERENCES

1. S. Lehoczky, F. R. Szofran and D. C. Gillies, Growth of solid solution single crystals. Second United States Microgravity Payload, Six Month Sciences Report, NASA MSC (1994).
2. B. N. Antar and V. S. Nuotio-Antar, *Fundamentals of Low Gravity Fluid Dynamics and Heat Transfer*. CRC Press, Boca Raton, FL (1993).
3. J. I. D. Alexander, Analysis of the low gravity tolerance of Bridgman–Stockbarger crystal growth—I. Steady and impulse accelerations. *Microgravity Sci. Technol.* **7**, 131 (1981).
4. J. I. D. Alexander, S. Amiroudine, J. Quazzani and F. Rosenberger, Analysis of the low gravity tolerance of Bridgman–Stockbarger crystal growth—II. Transient and periodic accelerations, *J. Crystal Growth* **113**, 21 (1991).
5. E. S. Nelson, An examination of anticipated g-jitter on space station and its effects on materials processes. NASA TM 103775 (1991).
6. D. Jacqmin, Stability of an oscillating fluid with a uniform density gradient, *J. Fluid Mech.* **219**, 449 (1990).
7. J. Casademunt, W. Zhang, J. Venals and R. F. Sekerka, Stability of a fluid surface in a microgravity environment, *AIAA Jl* **31**(11), 2027 (1993).
8. W. Zhang, J. Casademunt and J. Venals, Study of the parametric oscillator driven by narrow-band noise to model the response of a fluid surface to time-dependent accelerations, *J. Phys. Fluids A* **5**, 3147 (1993).
9. A. A. Wheeler, G. B. McFadden, B. T. Murray and S. R. Coriell, Convective stability in the Rayleigh–Benard and directional solidification problems: high frequency gravity modulation, *J. Phys. Fluids A* **3**, 2847 (1991).
10. J. I. D. Alexander, Residual gravity effects on fluid processes, *Microgravity Sci. Technol.* **2**, 131 (1994).
11. H. Chen, M. Z. Saghir, D. H. H. Quon and S. Chehab, Numerical study on transient convection in float zone induced by g-jitter, *J. Crystal Growth* **142**, 362 (1994).
12. S. Schneider and J. Straub, Influence of Prandtl number on laminar natural convection in a cylinder caused by g-jitter, *J. Crystal Growth* **97**, 235 (1989).
13. R. W. Series and D. T. J. Hurle, The use of magnetic fields in semiconductor crystal growth, *J. Crystal Growth* **113**, 305 (1991).
14. J. D. Jackson, *Classical Electrodynamics*. John Wiley and Sons, New York (1976).
15. S. Chandrasekhar, *Hydrodynamic and Hydromagnetic Stability*. Dover, New York (1961).
16. W. F. Hughes and F. J. Young, *The Electromagnetohydrodynamics of Fluids*. John Wiley and Sons, New York (1966).
17. W. Aung, Fully developed laminar convection between vertical plates heated asymmetrically, *Int. J. Heat Mass Transfer* **15**, 577–1580 (1972).
18. W. Aung and G. Worku, Theory of fully developed, combined convection including flow reversal, *J. Heat Transfer* **108**, 485 (1986).